

The Effect of Deformation Activation Volume, Strain Rate Sensitivity and Processing Temperature of Grain Size Variants

P. B. Sob, A. A. Alugongo, T. B. Tengen

Abstract—The activation volume of 6082T6 aluminum is investigated at different temperatures for grain size variants. The deformation activation volume was computed on the basis of the relationship between the Boltzmann's constant k , the testing temperatures, the material strain rate sensitivity and the material yield stress grain size variants. The material strain rate sensitivity is computed as a function of yield stress and strain rate grain size variants. The effect of the material strain rate sensitivity and the deformation activation volume of 6082T6 aluminum at different temperatures of 3-D grain are discussed.

It is shown that the strain rate sensitivities and activation volume are negative for the grain size variants during the deformation of nanostructured materials. It is also observed that the activation volume vary in different ways with the equivalent radius, semi minor axis radius, semi major axis radius and major axis radius. From the obtained results it is shown that the variation of activation volume increase and decrease with the testing temperature. It was revealed that, increase in strain rate sensitivity led to decrease in activation volume whereas increase in activation volume led to decrease in strain rate sensitivity.

Keywords—Nanostructured materials, grain size variants, temperature, yield stress, strain rate sensitivity, activation volume.

I. INTRODUCTION

DESPITE the great interest in severe plastic deformation (SPD) during past years, these deformation mechanisms are still uncertain [1]. Great research work with various SPD techniques and conditions gives different models for developed high angle boundaries (HABs) and structure refinement [1]. Some of the developed models extend the continuous evolution of dislocation structures by the crystallography glide from low and moderate strains. An alternative method describes the SPD as discontinuous due to localized flow inside shear bands (SBs) of non-crystallographic orientations [1]. Segal's [1] original contributions provoked the scientific community to transform the microstructure of a material deformed by SPD [2]. The grain sizes of the microstructure deformed by SPD vary due to the processing routes. The varying grain size has contributed

to the present controversy on nanomaterials mechanical properties [3].

The micro-mechanisms of size dependent strengthening are commonly explained by dislocation starvation effect application at nanoscale [4], [5]. High strain rate sensitivity (SRS) and low activation volume has been observed by [6]. Although nanoscale materials are being considered for different applications due to their enhanced mechanical properties, their rate limiting processes of activation volume remain "lack of deep understanding" that has called for many investigations now [6]. Most researchers have demonstrated the relationship between SRS and activation volume without taking into consideration the stochastic nature of grain size variants on the activation volume [7]-[14]. Most recent findings on the relationship between SRS and activation volume is only limited with the equivalent radius of the grain during grain refinement (with the equivalent radius defined as the radius of an equivalent sphere or cycle obtained by the displacement method of volume/area measurement). It is therefore necessary to model qualitatively the activation volume as a function of grain size variants during grain refinement. However the models of activation volume that dealt only with the equivalent radius ignored the stochastic nature of grain size variants during grain refinement. This current paper is aimed at studying the effect of processing temperature on the activation volume and grain size for 3-D grain deformed by Accumulative Roll-Bonding (ARB) and Equal Channel Angular Pressing (ECAP). The proposed models are tested with data from grain deformation in nanocrystalline aluminum samples.

II. METHODOLOGY

The characteristic equation of SRS which relates material yield stress ($\sigma(r)$) and strain rate ($\dot{\epsilon}$) is given by [7].

$$m = \frac{\log \left(\frac{\sigma(r_2)}{\sigma(r_1)} \right)}{\log \left(\frac{\dot{\epsilon}_2}{\dot{\epsilon}_1} \right)} \quad (1)$$

where $\sigma(r_1)$ and $\sigma(r_2)$ are the flow stresses corresponding to instantaneous strain rates $\dot{\epsilon}_1$ and $\dot{\epsilon}_2$, and $m = \text{SRS}$

The activation volume for plastic deformation which is directly related to the physical mechanism of deformation is given by [15]

P. B. Sob, A. A. Alugongo are with the Department of Mechanical Engineering, Faculty of Engineering and Technology, Vaal University of Technology, Vanderbijlpark 1900, Private Bag X021, South Africa (e-mail: baonhe_sob@rocketmail.com, alfayoa@vut.ac.za).

T. B. Tengen is with the Department of Industrial Engineering and Operations Management, Faculty of Engineering and Technology, Vaal University of Technology, Vanderbijlpark 1900, Private Bag X021, South Africa (e-mail: Thomas@vut.ac.za).

$$V = \frac{\sqrt{3}K_B T}{m(\sigma(r))} \quad (2)$$

where K_B is the Boltzmann constant, T temperature and m is the strain rate sensitivity. Equation (2) revealed that, the smaller activation volume the higher strain rate sensitivity. The activation volume as given in (2) is determined by a relationship of the values K_B , T , m and $\sigma(r)$. The strain rate sensitivity (m) varies with the increasing testing temperature on grain size variants. The dependence of the flow stress $\sigma(r)$ on the testing temperature T is ambiguous and differs during grain refinement. All these activities account for the complexity of the dependence of the activation volume value on the testing temperature.

The material yield stress $\sigma(r)$ on nanomaterial's grain subjected to plastic deformation is given by [16].

$$\sigma(r) = \sigma'_0 + A \left(r^{-\frac{1}{2}} \right) - B \left(r^{-1} \right) - C \left(r^{-\frac{3}{2}} \right) \quad (3)$$

where $\sigma'_0 = \sigma_0 + K_t$ is bulk yield stress, $A = K_d$ is HPR proportionality constant, $B = K_t [2hH_m / RT_r]$, $C = K_d [2hH_m / RT_r]$, K_t is a constant, h is atomic diameter in the case of metal, H_m is the bulk melting enthalpy, R is ideal gas constant, T_r is the room temperature, $K_d > 100K_t$ and $\sigma_0 > 10K_t$.

By employing the different models of strain (ϵ) for 3-D grain during grain refinement, the strain rate ($\dot{\epsilon}$) for r , r_1 , r_2 and r_3 during grain refinement are defined given as

$$d(\dot{\epsilon}_1) = \frac{d \left[\frac{dr_1}{r_1} \right]}{dt} = \frac{d \left(M \left(\frac{1}{r_{cl}} \right) \left(\frac{1}{r_1} \right) - \frac{1}{r_1^2} \right) dt + \frac{CDdW(t)}{r_1} - \frac{ZVr_1^2 d(t)}{r_1}}{dt} \quad (4)$$

where r_{cl} =local critical grain size, Z and D are Constants, $dW(t)$ =increment of the Wiener process, $V_1 = \tau_1 r_1^2$ define rate of grain breakage, $M = M_0 \left(1 + \frac{CD}{r_1} \right)$, $CD = 4(Hm)(h_0)/((k)(T))$, $T_m = T \{ \ln(m_{01}/m) \}$ and $M_0 = M_{01} \exp \{ -T_m(\ln f)/T \}$.

$$d(\dot{\epsilon}_3) = \frac{d \left[\frac{dr_3}{r_3} \right]}{dt} = \frac{d \left(\frac{Ratio_1 dr_1}{r_3} \right)}{dt} \quad (5)$$

$$d(\dot{\epsilon}_r) = \frac{d \left[\frac{dr}{r} \right]}{dt} = \frac{d \left(\frac{-Ord + IdW(t)}{r} \right)}{dt} \quad (6)$$

where O and I are constants

$$d(\dot{\epsilon}_2) = \frac{d \left[\frac{dr_2}{r_2} \right]}{dt} = \frac{d \left(\frac{Ratio_2 dr}{r_2} \right)}{dt} \quad (7)$$

Equations (1)-(7) are solved simultaneously using Engineering Equation Solver software (F-Chart Software, Madson, W153744, USA) and also employing the lognormal distribution of grain size [17].

III. RESULTS AND DISCUSSION

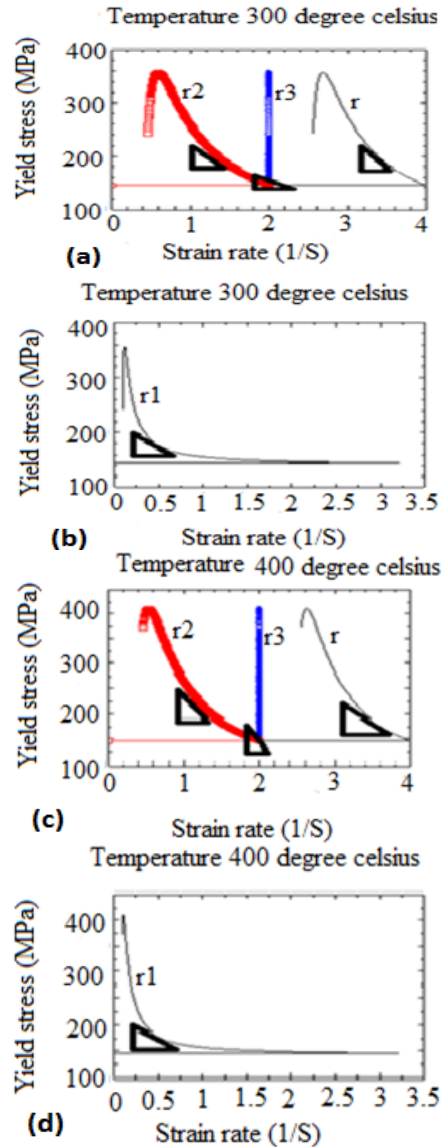


Fig. 1 (a)-(d) Plots of yield stress and strain rate at different temperatures and SRS calculated at the slops of the grain size variants. Some of the plots of yield stress and strain rate at different temperature and SRS calculated at the slops of the grain size variants are found in [19]

To test the models proposed in this report, the data from (nanocrystalline) aluminum sample (some of which are found in other reports: [18]) are used, $M_0' = 0.01 \text{ nm}^2 \text{ s}^{-1}$, $m = 4$, $CC = 12$, $a = 0.90$, $D = 10^{-4}$, $h_0 = 0.25 \text{ nm}$, $T_m(\infty) = 933.47 \text{ K}$, $CV_0 = 0.3$, $Ratio_1 = 0.81$, $Ratio_2 = 1.071$, $H_m(\infty) = 10.71 \text{ KJ Mol}^{-1}$, $\sigma_0' = 16.7 \text{ MPa}$, $K_t = 1.3$, $\sigma_0 = 15.40 \text{ MPa}$, $K_d = 1301.77 \text{ MPa nm}^{1/2}$, $R = 8.31 \text{ J K}^{-1} \text{ mol}^{-1}$, $T_r = 300 \text{ K}$, $K_B = 1.381023 \text{ J/K}$. The additional data obtained from this work are $O = 0.0035$, $I = 1.1$, $r_{cl} = 1.95r$,

$r_0=100nm$, $Z=0.4$ and $\tau_1 = 0.000008$. The additional data were obtained through curve fitting of the empirical data from the different measures of the sizes. The obtained results are presented in Figs. 1 (a)-(d), 2 and 3.

The SRS values at the grain size variants were calculated from the slopes of the plots at different temperature as the $d(\log(\sigma(r)))$ and $d(\log(\dot{\epsilon}))$, the activation volume were also calculated: these values are presented in Table I.

TABLE I
 THE RESULTS OF ACTIVATION VOLUME AND SRS MEASUREMENT AT SIX TEMPERATURES ON GRAIN SIZE VARIANTS

T(°C)	V(r ₁)	V(r ₂)	V(r ₃)	V(r)	(m) r ₁	(m) r ₂	(m) r ₃	(m) r
300	-45642.4	-45562	-43712	-29865.5	-5.66	-5.67	-5.91	-8.65
400	-70009.8	-63484.4	-88514.6	-33156.5	-5.74	-6.33	-4.54	-12.12
500	-89748.9	-28849.5	-112238.6	-27358.8	-6.13	-19.07	-2.83	-11.61
600	-219501.4	-148371	-160842	-156131	-3.40	-5.03	-4.64	-4.78
700	-202278	-179757	-202278	-49274	-4.47	-5.03	-4.47	-18.35
800	-275407	-275407	-237664	-237664	-4.03	-4.03	-4.67	-4.67

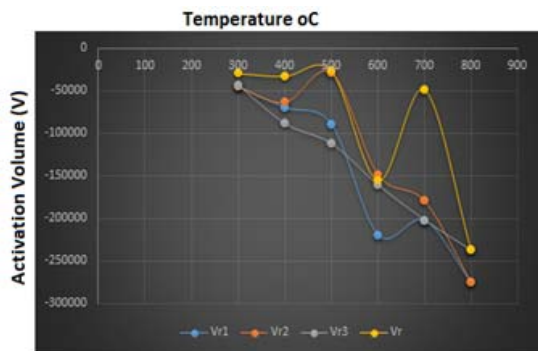


Fig. 2 Variation of activation volume (V) with Temperature at six temperatures within the negative activation volume range for temperature

IV. THE ACTIVATION VOLUME AND TEMPERATURE

The variation of activation volume with temperature is shown in Fig. 2 for six temperatures. It is observed that, at a temperature range from room-temperature up to 400°C, no pronounced activation volume is found for r whereas the activation volume decreased along r₂, r₁ and r₃. By increasing the testing temperature further, the activation volume also increased and decreased on grain size variants. The different results of activation volume on grain size variants are due to different grain curvatures during grain refinement. The higher amount of high angle grain curvatures is the main reason for the lower activation volume and the lower amount of low angle grain curvatures is the main reason for a high activation volume on grain size variants. The above results indicate a change in the activation volume during grain refinement on the grain size variants due to different grain curvatures. It is however noted that, the activation volume characterizes the stress sensitivity of dislocation velocity which is related with the dislocation process of different grain curvatures of the grain size variants. It is also based on the thermally activated plastic deformation process of the grain curvature of the grain

size variants. The dislocation velocity depend on the activation energy and also the shear stress acting on the dislocation which is characterized by different grain curvatures on the grain size variants during grain refinement.

Looking at the effect of curvature on activation volume, it is observed from Fig. 2 that, at a temperature of 400°C different activation volume are revealed for the grain size variants. From the different activation volume revealed at a temperature of 400°C the material activation volume is lower for radius measured along r₃ since the grain curvature for r₃ is higher when compared with the curvatures of r₂ and r₁. When the testing temperature increased from 400°C to 500°C the activation volume is still lower along r₃ and r₁ increased along r₂ and r since the grain curvature of r₃ and r₁ is higher when compared with the curvatures of r₂ and r. The increased in activation volume with increased in testing temperature could also be rationalized based on the fact that during grain refinement of 6082T6 aluminum there is the martensitic (crystal structure) state. And the grain size variants are characterized with lower grain curvature. It has been revealed that, the SRS tends to increase with temperature on grain size variants due to higher grain curvature, whereas the effect of temperature on activation volume decreased with higher grain curvature, the obtained results is similar to that observed by [15].

V. THE ACTIVATION VOLUME (V) AND GRAIN SIZE VARIANTS

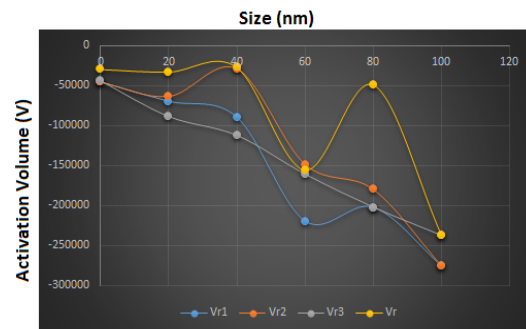


Fig. 3 Variation of activation volume (V) with Size (nm) at six temperatures within the negative activation volume range for grain size variants

The main reasons for the increased and decreased in activation volume is due to different grain curvatures on the grain size variants as already explained. It is observed from Fig. 3 that the activation volume vary with grain size variants due to different grain curvatures. It is observed from Fig. 3 that at a grain size of 20nm different activation volume are revealed for the grain size variants. From the different activation volume revealed at a grain size of 20nm the activation volume is lower for radius measured along r₃, r₁ and r₂ whereas it is higher along r since the grain curvature of r is lower than the curvatures of r₃, r₁ and r₂. It is observed at a grain size of 40nm that, the activation volume decreased when measured along r₃ and r₁ whereas it increased along r and r₂ due to higher grain curvatures of r₃ and r₁ and lower grain

curvature of r and r_2 . It is also observed at a grain size of 60nm to 80nm that, the activation volume increased along r and decreased along r_1 , r_2 and r_3 . It is further observed at a grain size of 100nm that the activation volume decreased along r , r_1 , r_2 and r_3 . The results in Fig. 3 revealed increased and decreased of activation volume due to different grain curvature on grain size variants. However the smooth transition of grain size variants at different temperatures cannot be under looked as the obtained results revealed transition at different temperature from negative activation volume as temperature increased on the grain size variants.

VI. CONCLUSIONS

The current work was aimed at studying the effect of processing temperature on activation volume for grain size variants. To achieve that, the model of activation volume for plastic deformation which is directly related to the physical mechanism of deformation given by [15] was modified to be applicable to 3-D grain. The model of SRS was also modified to be applicable to 3-D grain. The stochastic natures of the grain size variants were also taken into consideration.

It can be concluded that, the activation volume characterizes the stress sensitivity of dislocation velocity which is related with the dislocation process during grain refinement. This is also based on the thermally activated plastic deformation process of grain size variants, the dislocation velocity also depend on the activation energy and the shear stress acting on the dislocation. These activities are characterized by different grain curvatures of grain size variants during grain refinement.

The effect of deformation temperature led to different activation volume due to different grain curvatures on the grain size variants. It was also observed that the activation volume of the grain size variants decreased and increased with increasing temperature. It can also be concluded that, increased in SRS led to decrease in activation volume whereas increased in activation volume led to decrease in SRS due to different grain curvature.

ACKNOWLEDGMENT

The National Research Foundation (NRF) and Vaal University of Technology (VUT) base this material on the work which is supported financially.

REFERENCE

- [1] Segal, V. M. 2005. Deformation mode and plastic flow in ultra-fine grained metals. *Materials Science and Engineering A* 406(2005)205-216.
- [2] Laszlo, S. Toth & Chengfan Gu. Ultrafine grain metals by severe plastic deformation. *Material Characterization* 92(2014) 1-14.
- [3] Cuenot, S. & Fretigny, C. & Demoustier, S. & NYSTEN, B. 2004. Surface tension effect on the mechanical properties by atomic microscopy. *The American Physical Society* 69 (16):1-5, 20.
- [4] Wang, Z. J. & Shan, Q. J. & Sun, L. J. & MA, E. 2012. Sample size effects on the large strain bursts in submicron aluminum pillars. *Applied Physics Letters* 100, 071906.
- [5] Zhou, C. & Beyerlein, I. J. & LESAR, R. 2011. Plastic deformation mechanisms of fcc single crystals at small scales. *Acta Materialia* 59 (20), 7673-7682.
- [6] Zhu, T. & LI, J. & Samanta, A. & Leache, A. & Gall, K. 2008. Temperature and strain rate dependence of surface dislocation nucleation. *Physical Review Letters* 100 (2), 025502.
- [7] Anton, S. & Brane, S. & Mateyz, F. 2009. Determination of the strain-rate sensitivity and the activation energy of deformation in the superplastic aluminium alloy Al-Mg-Mn-Sc. *RMZ – Materials and Geoenvironment, Vol. 56, No. 4, pp. 389–399, 2009.*
- [8] Sabirov, I. & Barnett, M. R. & Estrin, Y. & Hodgson, P. D. 2009. The effect of strain rate on the deformation mechanisms and the strain rate sensitivity of an ultra-fine-grained Al alloy. *Scripta Materialia* 61 (2009) 181–184.
- [9] Brad, L. B. & Thomas, B. C. & Morris, F. D. 2007. The Strain-Rate Sensitivity of High-Strength High-Toughness Steels. *Sanddia Report Sand 2007-0036.*
- [10] Kumar, R. & Sharma, G. & Kumar, M. 2013. Effect of size and shape on the vibrational and thermodynamics properties of nanomaterials. *Journal of thermodynamics* Vol. pp 5.
- [11] Lee, W. S. & Lin, C. F. & Chen, T. H. & Hwang, H. H. 2008. Effects of strain rate and temperature on mechanical behavior of Ti–15Mo–5Zr–3Al alloy. *J Mech Behav Biomed Mater* 2008;1(4):336–44.
- [12] Chiou, S. T. & Tsai, H. L. & Lee, W. S. 2009. Impact mechanical response and microstructural evolution of Ti alloy under various temperatures. *J Mater Process Technol* 2009; 209(5):2282–94.
- [13] Guisbiers, G. 2010. Size dependent materials properties towards a universal equation. *Nanoscale Research Letters, Vol. 5, No.7, pp. 1132–1136.*
- [14] Zhang, Z. & Lii, X. X. & Jiang, Q. 1999. Finite size effect on melting enthalpy and melting entropy of nanocrystals. *Physical B Vol. 270, No. 3-4, pp. 249-254.*
- [15] Gunderov, D. V. & Maksutova, G. & Churakova, A. & lukyanov, A. & Kreitberg, A. & Raab, G. I. & Sabirov, A. I. & Prokoshkin, S. 20015. Strain rate sensitivity and activation volume of coarse-grained and ultrafine-grained TiNi alloys. *Scripta Materialia* 102 (2015) 99-102.
- [16] Zhao, M. & Jiang, Q. 2006. Reverse hall-petch relationship of metals in nanometer size. *Emerging Technologies-Nanoelectronics, IEEE Conference on Vol. pp 472-474, (10-13 Jan. 2006.*
- [17] Tengen, T. B. & Iwankiewicz, R. 2009. Modelling of the grain size probability distribution in polycrystalline. *Composite Structures* 91(2009) 461-466
- [18] Tengen, T. B. 2008. *Analysis of Characteristic of Random Microstructures of Nanomaterials.* PhD. Thesis. Witwatersrand Johannesburg.
- [19] Sob, P. B. & Alugongo, A. A. & Tengen, T. B. 2015. *Determination of strain rate sensitivity (SRS) for grain size variants on nanocrystalline materials produced by ARB and equal channel angular pressing (ECAP).* 17th International Conference on Advanced Materials and Nanotechnology (ICAMN 2015), World Academy of Science, Engineering and Technology, Bangkok, Thailand, paper number 15TH12000585.